Photosensitivity of Nb_2O_5/Si Thin Films Produced via DC Reactive Sputtering at Different Substrate Temperatures

Yahya R. Hathal [1]
Isam M. Ibrahim [1]
Mohammed K. Khalaf [2]

[1] *Department to Physics, College of Science, University of Baghdad, Baghdad, IRAQ*
[2] *Department of Materials Research, Ministry of Science and Technology, Baghdad, IRAQ*

This study thoroughly investigates the potential of niobium oxide (Nb_2O_5) thin films as UV-A photodetectors. The films were precisely fabricated using dc reactive magnetron sputtering on Si(100) and quartz substrates, maintaining a consistent power output of 50W while varying substrate temperatures. The dominant presence of hexagonal crystal structure Nb_2O_5 in the films was confirmed. An increased particle diameter at 150°C substrate temperature and a reduced Nb content at higher substrate temperatures were revealed. A distinct band gap with high UV sensitivity at 350 nm was determined. Remarkably, films sputtered using 50W displayed the highest photosensitivity at 514.89%. These outstanding optoelectronic properties highlight Nb_2O_5 thin films' potential for use in optoelectronic circuits and UV-A sensors, especially in the visible-blind range. These findings underscore Nb_2O_5 thin films' promise in advancing UV-A photodetector technology.

Keywords: Nb_2O_5 thin film; Substrate temperatures; Sputtering; Photosensitivity
Received: 23 January 2024; **Revised:** 27 February; **Accepted:** 05 March 2024

1. Introduction

Metal oxide thin films have gained significant prominence across various fields, including optics and microelectronics. Among these materials, niobium oxide (Nb_2O_5) stands out as a highly sought-after transparent conducting oxide. Its distinct electronic and optical properties render it a compelling choice for a wide range of electronic and optical applications [1]. Nb_2O_5, classified as an n-type transition material, has undergone extensive exploration due to its versatility in applications such as gas sensors, catalysts, dye-sensitized solar cells (DSSCs), displays, and optical coatings. Its appeal lies in its favorable attributes, including remarkable thermal stability, corrosion resistance, high refractive index, and notably, a wide band gap [2-4]. In the electromagnetic spectrum, UV light encompasses higher frequencies beyond the human eye's visible range. UV radiation spans from 200 to 400 nm, with the sun serving as a primary source. While a significant portion of the UV spectrum, particularly the ultraviolet-C (UV-C) region (200-290 nm), and a substantial part of the UV-B region (290-320 nm), are absorbed by atmospheric molecules and sunscreens, the longer wavelengths in the UV-A band (320-400 nm) penetrate the Earth's surface. Prolonged exposure to UV-A radiation poses health risks, including an increased the possibility of skin cancer [5]. Therefore, efficient techniques for monitoring UV-A radiation are essential. Numerous methods have been employed to produce Nb_2O_5 thin films, encompassing dc magnetron sputtering, ion beam sputtering, electron beam evaporation, thermal oxidation, photochemical vapor deposition, plasma-enhanced chemical vapor deposition, spray pyrolysis, sol-gel techniques, and pulsed laser deposition [6-10]. Among these methods, sputtering stands out for its ability to produce thin films of diverse materials, including oxides [11-15]. Renowned for its capacity to deposit thin films with exceptional uniformity, homogeneity, density, purity, adhesion, and reproducibility at a high deposition rate, sputtering is highly regarded in the thin film deposition realm [16-21]. This technique facilitates consistent film thickness over extensive substrate areas and is readily accessible through commercially available sputtering systems [22-26]. The resultant thin films exhibit remarkable transparency and conductivity [27-30].

The present investigation endeavors to pinpoint the optimal substrate temperature for producing Nb_2O_5/Si thin films exhibiting maximum photosensitivity. The study scrutinizes the influence of substrate temperatures on various film properties, including structural, morphological, optical characteristics, and sensing capabilities. The insights gleaned from this research hold the potential to enhance the efficacy of photosensitive devices, unlocking new possibilities in the realm of UV-A radiation monitoring.

2. Experimental Work

This study aimed to investigate the substrate temperature impact on the microstructure, optical and electrical properties of niobium oxide (Nb_2O_5) thin films. This material was deposited on quartz substrate to evaluate their structural, morphological, optical, and electrical characteristics. The deposition process was carried out using a dc reactive magnetron technique with a consistent power output of 50W. The

sputtering target utilized 99.95% pure niobium disk with a 5 cm diameter and 3 mm thickness.

Firstly, the quartz substrates have been cleaned by soaking them in ultrasonic bath of isopropanol and deionized water, followed by drying with nitrogen gas. The sputtering process involved argon (Ar) gas (99.99%) as the sputtering gas and oxygen gas as the reactive gas. The vacuum chamber was evacuated at $4.2x10^{-5}$ mbar using a diffusion pump. The flow rate of the Ar gas during sputtering process was maintained at a constant 50 sccm. While the O_2 flow rate was 5 sccm. The deposition process performed for 120 minutes. Subsequently, the deposited thin films annealed at 800°C for one hour in an ambient air.

The x-ray diffraction (XRD) patterns were analyzed using a Shimadzu XRD-6000 x-ray diffractometer with CuK_α radiation (0.154 nm) in the 2θ range from 10° to 90°. The samples' crystal structure and surface morphology were observed using field-emission scanning electron microscopy (FE-SEM), and statistical and image analyses were conducted using Image J and Origin LAB. The optical absorption spectra and optical energy gap of the deposited thin films in the 300-1100 nm wavelength range were determined using a Shimadzu UV-1650 PC UV-Visible spectrophotometer. Light sensitivity measurements were performed using Sensible Fluke 8846A digital electrometers.

3. Results and Discussion

The XRD patterns of Nb_2O_5 thin film samples that fabricated under a constant dc power of 50W with variant substrate temperatures (room temperature, 100°C and 150°C), are illustrated in Fig. (1). The result shows that all samples exhibited the presence of a hexagonal Nb_2O_5 structure. Elevating the substrate temperature notably enhanced the crystallinity of the samples. Such as, the sample fabricated with 50W DC power and substrate temperature of 150°C displayed the highest degree of crystallinity. This is an evidence of presence four distinct peaks corresponding to the (001), (100), (101), and (002) lattice planes, discernible at 2θ= 22.38°, 28.52°, 36.76° and 46.11°, respectively [31]. These observed peaks were found to align with JCPDS card no. 00-028-0317. Furthermore, the elevation of substrate temperature resulted in narrower diffraction lines, signifying larger crystallite sizes. This phenomenon can be attributed to the increased thermal energy at higher temperature, allowing atoms to arrange themselves more effectively during the thin film growth process and reducing the grain boundaries [32-34]. The increase of substrate temperature also reduced crystal defects, dislocations and lattice strain caused by the nano-size effect. The assessment of crystallite size was performed using the Scherrer's formula, with focus on the (001) crystal plane. The results revealed that crystallite size ranged from 21.7 to 26.0 nm, with an increase in substrate temperature from room temperature to 150°C. Table (1) provides comprehensive data on the measured crystallite sizes corresponding to the most prominent peaks, including peak positions, Miller indices and full-width at half maximum (FWHM) values [35]. These XRD findings underscore the significant influence of substrate temperature on the crystalline properties of Nb_2O_5 thin films, offering valuable insights into the structural characteristics of the materials under investigation.

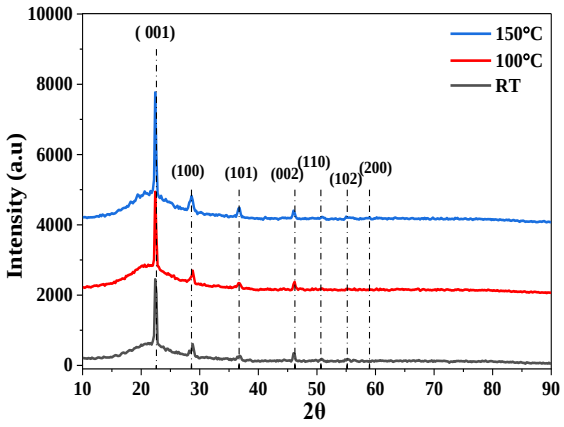

Fig. (1) XRD patterns of Nb_2O_5 thin films deposited at various substrate temperatures using 50W DC power

Equation (1) can be used to compute the absorption coefficient for the frequency associated with the highly absorbent region. This involves using the values of absorption (A) and thickness (t) to derive the coefficient:

$$\alpha = 2.303\frac{A}{t} \quad (1)$$

Both crystalline and amorphous materials exhibit distinct and noticeable characteristics in their fundamental absorption edges. Before determining the band gap of the material, it is crucial to understand the transition from the valence band to the conduction band. The energy band gap (E_g) can be calculated using Eq. (2) [36]

$$\alpha h\nu = B(h\nu - E_g)^r \quad (2)$$

The optical absorption coefficient (α) is determined by various factors, including the optical energy gap (E_g), the material structure (β) and the index (r) that describes the optical absorption process, according to the provided equation [37,38]. The absorption-causing electronic transition's r-coefficient was 0.5

Our results show good agreements with previous studies, demonstrating direct optical transitions [39]. The optical absorbance curves of Nb_2O_5 thin films fabricated using a constant dc power of 50W at various substrate temperatures (RT, 100, and 150 °C) in the wavelength range of 200–800 nm are presented in Fig. (2). It can be observed that the films exhibit high transparency in the visible region. As the substrate temperature increased, there was a decrease in absorbance, which can be attributed to the reduction of defects. This improvement in

crystallinity and reduction in optical scattering at grain boundaries contributed to the reduced absorbance [40].

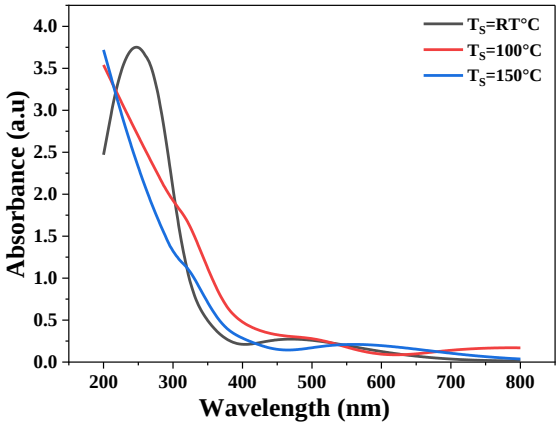

Fig. (2) UV-visible spectra of Nb_2O_5 thin films fabricated using 50W DC power at different substrate temperatures

Usually, the optical band gap variations are attributed to the Moss-Burstein shift, a phenomenon commonly referred to as a blue shift. This shift is typically a result of an increased carrier concentration stemming from the filling of the optical band. Conversely, a redshift, characterized by a decrease in the optical band gap, is believed to be induced by many-body effects, including interactions between electrons and electrons or impurities, leading to an excessive density of donors surpassing a certain threshold [41].

Figure (3) presents the relationship between the square of the product of the optical absorption coefficient (α) and photon energy (hν) for Nb_2O_5 thin films generated using a 50W dc power source at various substrate temperatures. The outcomes revealed an escalation in the energy gap from 3.93 to 4.60 eV as the substrate temperature increased from room temperature to 150°C. This increase in substrate temperature corresponds to a rise in the oxygen content within the deposited thin film. As the oxygen content increases, the presence of oxygen vacancies within the film decreases. The variation in oxygen content with changing substrate temperature directly influences the energy band gap of the thin film. Specifically, an increase in oxygen content can lead to an expansion of the energy bandgap. This effect is attributed to the role of oxygen atoms as electron acceptors, contributing to the widening of the energy gap between the valence and conduction bands [42].

In summary, the observed changes in the optical band gap of Nb_2O_5 thin films can be attributed to alterations in oxygen content induced by varying substrate temperatures. These findings shed light on the connection between material composition and optical properties, offering insights into the potential applications of these thin films in optoelectronic devices.

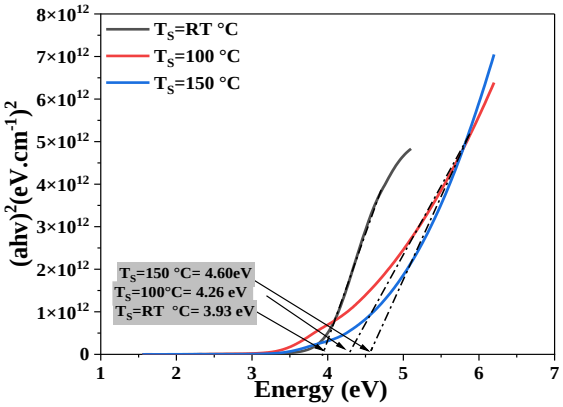

Fig. (3) Variation of $(\alpha h\nu)^2$ with $(h\nu)$ for Nb_2O_5 thin films deposited using 50W dc power at different substrate temperatures

The FE-SEM images presented in Fig. (4) provide a comprehensive view of the surface morphology of Nb_2O_5 thin films. These films were meticulously deposited onto quartz slide substrates under controlled temperatures, namely room temperature (RT), 100°C and 150°C, while maintaining a constant sputtering power of 50W. Examination these images reveal a distinct trend highlighting the influence of substrate temperature on the structural characteristics of the thin films.

The substrate temperature significantly influences thin film deposition and particle size distribution from a physics perspective. As substrate temperatures rise, the thermal energy of atoms on the substrate surface increases significantly. According to statistical mechanics, the elevated thermal energy enhances atomic diffusion, allowing atoms from the sputtered material to move more freely across the substrate surface. This enhanced atomic mobility that plays a pivotal role in the formation of smaller particles during thin film deposition, as atoms have a higher probability of encountering each other and forming bonds at shorter distances. These principles are governed by Fick's laws of diffusion, which describes the particles dispersion through a medium over time [43]. Additionally, substrate temperature impacts the nucleation and growth processes of thin films. Nucleation refers to the initial formation of particles, while growth involves their subsequent increase in size [44].

The increased thermal energy promotes the mobility of atoms, leading to a higher rate of nucleation. Importantly, the growth rate remains moderate, resulting in the formation of smaller and more uniform size of particles.

However, at higher substrate temperatures, such as 150°C, the elevated thermal energy not only boosts nucleation but also accelerates growth. This behavior aligns with classical nucleation and growth theory and is consistent with the principles of statistical physics [45].

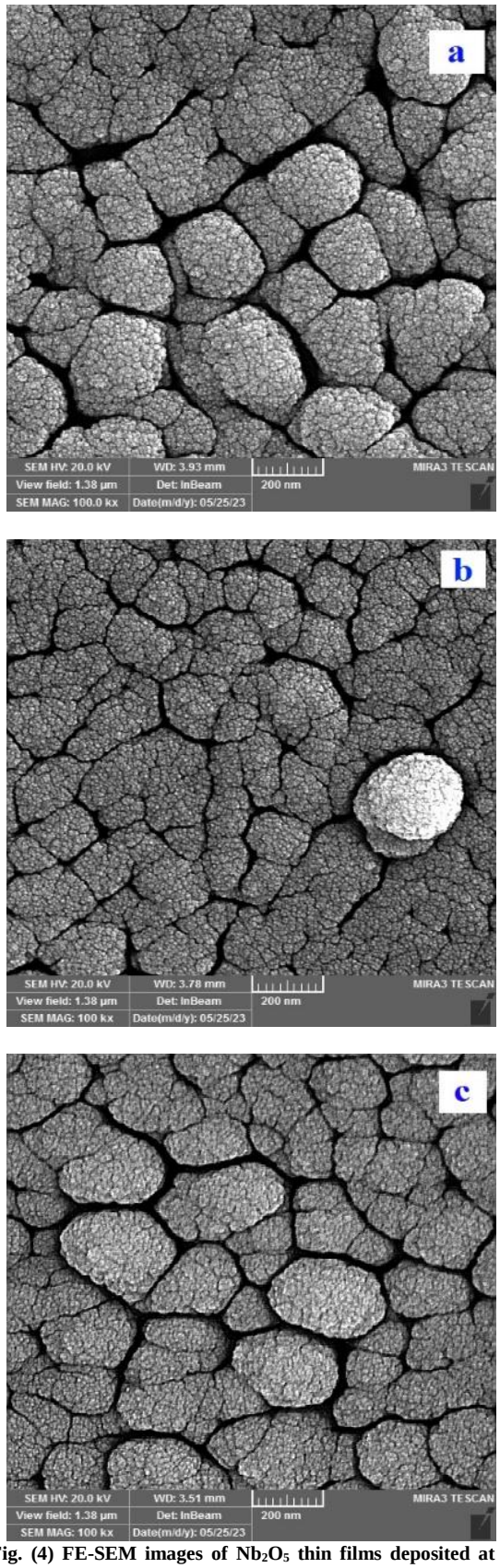

Fig. (4) FE-SEM images of Nb_2O_5 thin films deposited at a constant dc power of 50W and different substrate temperatures: (a) RT, (b) 100°C, and (b) 150°C

Figure (5) illustrates the EDX spectra of Nb_2O_5 thin films deposited on quartz slide substrates at various temperatures (RT, 100, and 150°C) using a dc sputtering power of 50W. These spectra exhibit multiple peaks corresponding to the emission lines of oxygen (O) and niobium (Nb). Notably, an increase in substrate temperature leads to higher oxidation levels, resulting in an elevated oxygen concentration from 80.5 at.% to 94.2 at.% and a decrease in Nb concentration from 19.5 at.% to 5.8 at.%. This process potentially reduces the number of electron vacancies, leading to a decline in the concentration of charge carriers [46]. Excess oxygen beyond its stoichiometric ratio on the surface of nanoparticles can be attributed to the presence of adsorbed oxygen species originating from the surrounding environment. Additionally, the EDX spectrum displays a distinct peak at 1.75 eV, corresponding to silicon emissions. This peak serves as an indicator of the quartz (SiO_2) substrate employed in the deposition process, highlighting the thoroughness of the elemental analysis.

The I-V characteristics are important parameter for assessing heterojunctions, representing the current response under different forward and reverse biases in both dark and light conditions. Figure (6) illustrates the typical I-V characteristics of Nb_2O_5 thin films fabricated on p-type Si (100) substrates at a constant power of 50 W at RT, 100°C, and 150°C. The I-V measurements were performed under various light intensities showing an increase of photocurrent with higher light intensity. The experiment involved a voltage sweep from -1 to 1 V. The I-V characteristics exhibit two types of currents: the forward dark current which driven by majority carriers and the recombination current which occurring at lower voltages due to the concentrations of majority and minority carriers exceeding the intrinsic carrier concentration ($n_i^2<np$). Additionally, a small increase of recombination current observed at low voltage regions which attributed to electron excitations from the valence band (V.B) to the conduction band (C.B). As voltage increases, the diffusion current dominates, resulting in an exponential increase in current magnitude [47]. On the other hand, the decrease of reverse bias current with increasing substrate temperature in Nb_2O_5 thin films which can be attributed to the reduction of interface states and trap levels at the metal/semiconductor interface that leading to improve Schottky barrier height (SBH) and ideality factor (IF) of the metal/Nb_2O_5 contact. This reduction in trap levels and interface states at higher temperatures can be attributed to improve crystallinity, reduced oxygen vacancies in the Nb_2O_5 thin films and decreased roughness of the Nb_2O_5 surface. Consequently, more uniform and defect-free Nb_2O_5/Si interface is achieved, resulting in a decrease in reverse bias current.

Figure (7) illustrates the time-dependent photosensitivity characteristics of Nb_2O_5 thin films excited with UV light of 350 nm wavelength and an intensity of 0.0004 W/cm². The samples were fabricated at RT, 100°C and 150°C. The dark current

values the films were measured at 0.038, 0.028, and 0.013 μA, respectively. Upon UV illumination, the photocurrent significantly exceeded the dark current, surpassing it by a factor of over ten. The light sensitivity of Nb_2O_5 thin films was assessed using Eq. (3):

$$S = \frac{I_{PH}-I_d}{I_d} \times 100\% \quad (3)$$

where I_{ph} represents the photocurrent and I_d represents the dark current. This evaluation yielded a sensitivity of 514.89% at a substrate temperature of RT

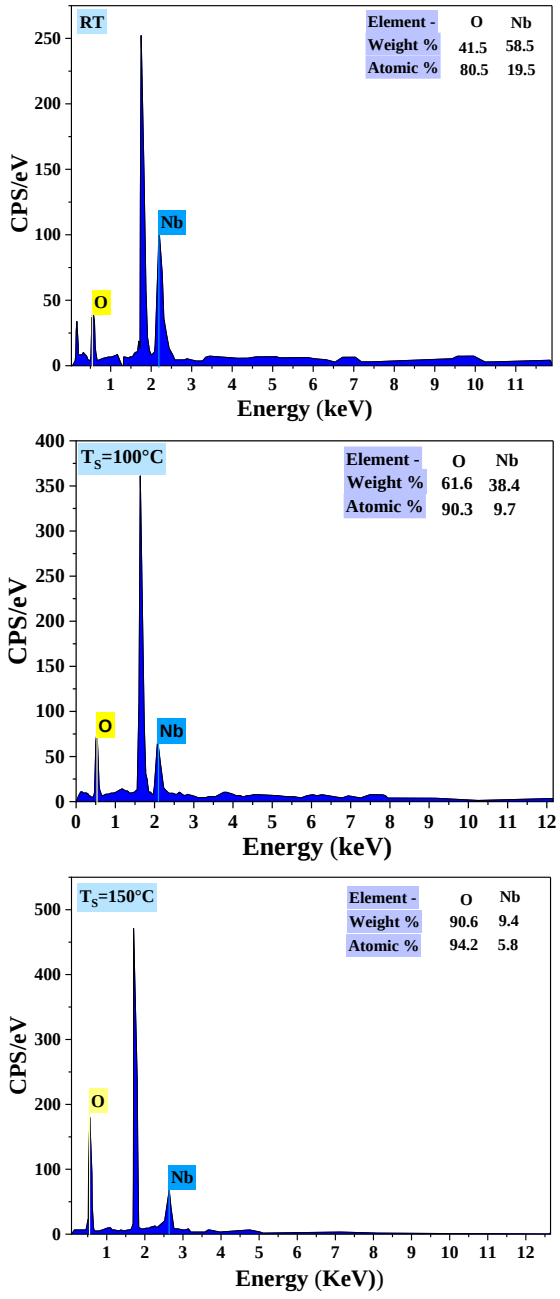

Fig. (5) EDX spectra of Nb_2O_5 thin films fabricated using 50W dc power at different substrate temperatures

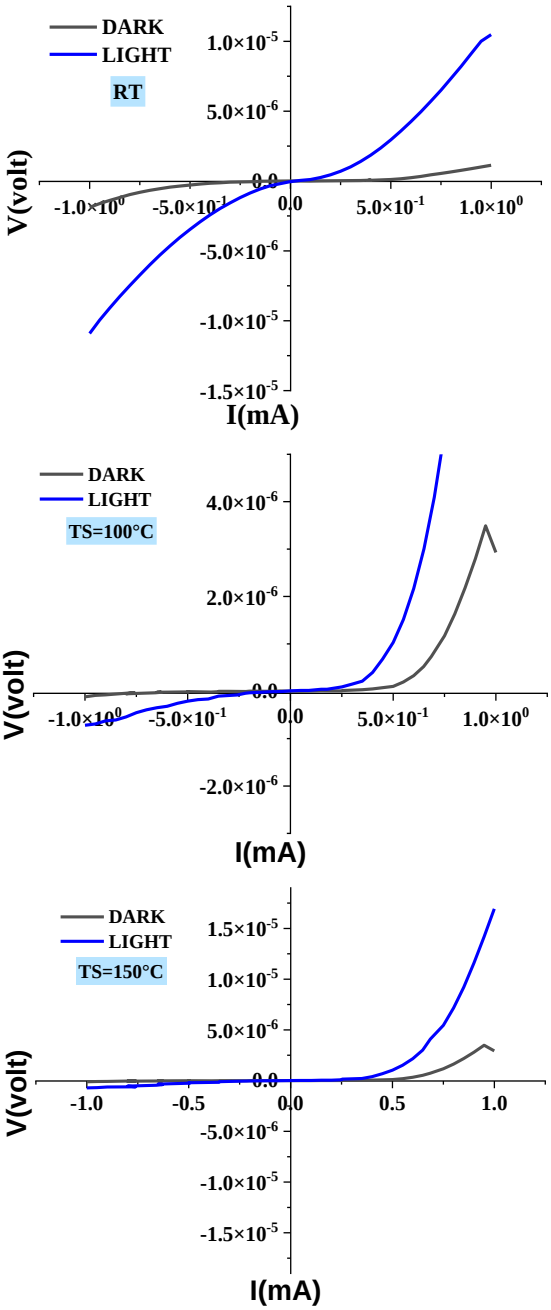

Fig. (2) Dark and illumination I-V characteristics of Nb_2O_5 thin films fabricated using 50W dc power at different substrate temperatures (RT, 100 °C, and 150 °C)

Interestingly, as the substrate temperature was gradually increased from RT to 100°C, light sensitivity exhibited a consistent decrease, reaching its maximum value of 244.71% at 100°C. However, at a substrate temperature of 150°C, the sensitivity experienced a decline to 67.63%.

The primary observation of significant importance is the notably heightened level of photosensitivity demonstrated by the UV sensor when employing the sample growth under constant sputtering power conditions of 50W and a substrate temperature at RT. This enhanced performance can be attributed to the distinct attributes inherent to the film produced under RT conditions. The film displays reduced reflectance

spectra in the UV range, a quality that holds considerable advantages in the domain of photodetection devices.

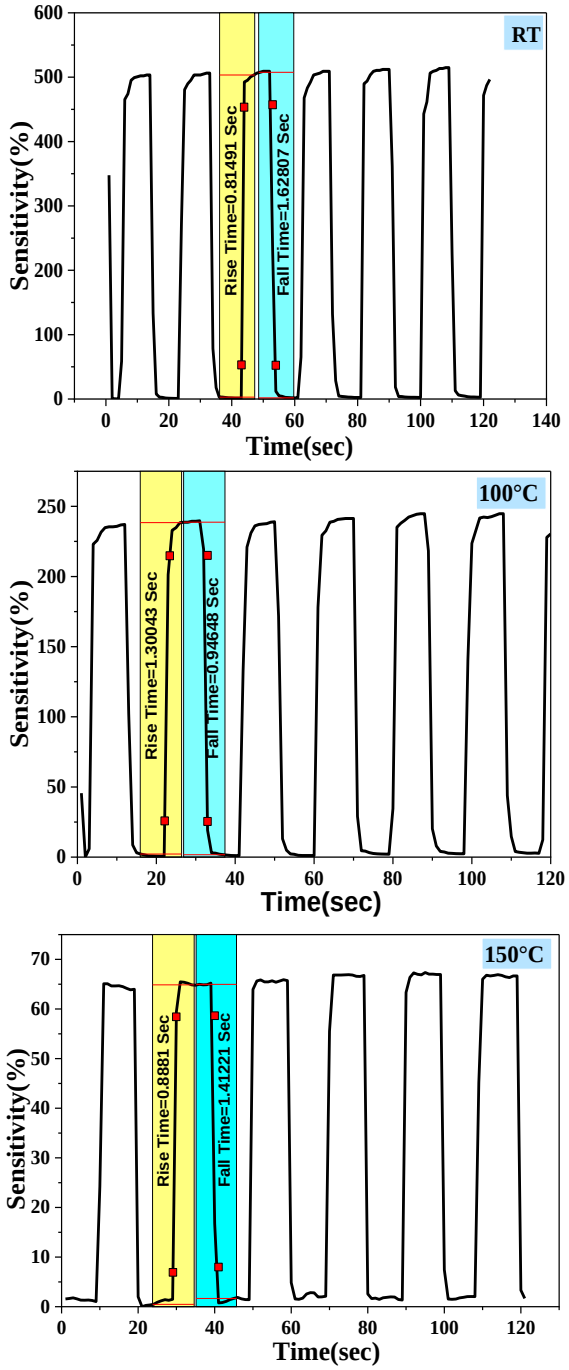

Fig. (7) Time-dependent photosensitivity of Nb_2O_5 thin films deposited using dc power of 50W at RT, 100 °C, and 150 °C

The reduction in sensitivity as the deposition temperature increases is not an arbitrary outcome. Instead, it can be rationalized by the elevated temperatures' ability to induce a heightened degree of reflectivity within the film, particularly in the UV spectrum. This amplified reflectance phenomenon functions to restrict the amount of UV radiation absorbed by the film, consequently resulting in the reduction of photo-induced charge carrier generation, the very essence of photosensitivity [48].

4. Conclusions

This research achieved a successful deposition of high-quality Nb_2O_5 thin films onto quartz substrates. Well-defined polycrystalline hexagonal structures in the Nb_2O_5 thin films were confirmed, a finding consistently observed across varying substrate temperatures. Moreover, a noticeable increase in particle size and stronger inter-particle connectivity of substrate temperature at 150°C was revealed. Notably, an escalation in dc power correlated with an increase in the direct optical energy gap. Furthermore, a decrease in Nb content with rising substrate temperature was observed. This investigation extended to the deposition of Nb_2O_5 thin films on silicon wafers and results demonstrated a swift and substantial response to UV light at 350nm, showcasing an impressive photosensitivity rating of 514.89% upon exposure.

References

[1] N.C. Emeka, P.E. Imoisili and T.C. Jen, "Preparation and Characterization of Nb_xO_y Thin Films: A Review", *Coatings*, 10(12) (2020) 1246.

[2] M. Mazur et al., "Determination of optical and mechanical properties of Nb_2O_5 thin films for solar cells application", *Appl. Surf. Sci.*, 301 (2014) 63-69.

[3] R.A. Rani et al., "Nanoporous Nb_2O_5 hydrogen gas sensor", *Sens. Actuat. B: Chem.*, 176 (2013) 149-156.

[4] Ö.D. Coşkun and S. Demirela, "The optical and structural properties of amorphous Nb_2O_5 thin films prepared by RF magnetron sputtering", *Appl. Surf. Sci.*, 277 (2013) 35-39.

[5] X. Fang et al., "New ultraviolet photodetector based on individual Nb_2O_5 nanobelts", *Adv. Func. Mater.*, 21(20) (2011) 3907-3915.

[6] R. Panetta et al., "Synthesis and characterization of Nb_2O_5 mesostructures with tunable morphology and their application in dye-sensitized solar cells", *Mater. Chem. Phys.*, 202 (2017) 289-301.

[7] R. Chandrasekharan et al., "Thermal oxidation of tantalum films at various oxidation states from 300 to 700°C", *J. Appl. Phys.*, 98(11) (2005).

[8] J.P. Masse et al., "Stability and effect of annealing on the optical properties of plasma-deposited Ta_2O_5 and Nb_2O_5 films", *Thin Solid Films*, 515(4) (2006) 1674-1682.

[9] H. Szymanowski et al., "Optical properties and microstructure of plasma deposited Ta_2O_5 and Nb_2O_5 films", *J. Vac. Sci. Technol. A: Vac. Surf. Films*, 23(2) (2005) 241-247.

[10] S.H. Mujawar et al., "Electrochromic properties of spray-deposited niobium oxide thin films", *Solid Stat. Ion.*, 177(37-38) (2006) 3333-3338.

[11] M.K. Khalaf et al., "Operation Characteristics of a Closed-Field Unbalanced Dual-Magnetrons Plasma Sputtering System", *Bulg. J. Phys.*, 41(1) (2014) 24-33.
[12] M.K. Khalaf et al., "Effect of Adding Nitrogen to the Gas Mixture on Plasma Characteristics of a Closed-Field Unbalanced DC Magnetron Sputtering System", *Iraqi J. Appl. Phys.*, 10(1) (2014) 27-31.
[13] M.K. Khalaf et al., "Fabrication of UV Photodetector from Nickel Oxide Nanoparticles Deposited on Silicon Substrate by Closed-Field Unbalanced Dual Magnetron Sputtering Techniques", *Opt. Quant. Electron.*, 47(12) (2015) 3805-3813.
[14] M.K. Khalaf et al., "Fabrication and Characterization of UV Photodetectors Based on Silicon Nitride Nanostructures Prepared by Magnetron Sputtering", *Proc. IMechE, Part N, J. Nanomater. Nanoeng. Nanosys.*, 230(1) (2016) 32-36.
[15] M.K. Khalaf et al., "Silicon Nitride Nanostructures Prepared by Reactive Sputtering Using Closed-Field Unbalanced Dual Magnetrons", *Proc. IMechE, Part L, J. Mater.: Design & Appl.*, 231(5) (2017) 479-487.
[16] M.A. Hameed and Z.M. Jabbar, "Preparation and Characterization of Silicon Dioxide Nanostructures by DC Reactive Closed-Field Unbalanced Magnetron Sputtering", *Iraqi J. Appl. Phys.*, 12(4) (2016) 13-18.
[17] F.J. Al-Maliki and E.A. Al-Oubidy, "Effect of gas mixing ratio on structural characteristics of titanium dioxide nanostructures synthesized by DC reactive magnetron sputtering", *Physica B: Cond. Matter*, 555 (2019) 18-20
[18] B.K. Nasser and M.A. Hameed, "Structural Characteristics of Silicon Nitride Nanostructures Synthesized by DC Reactive Magnetron Sputtering", *Iraqi J. Appl. Phys.*, 15(4) (2019) 33-36.
[19] S.H. Faisal and M.A. Hameed, "Heterojunction Solar Cell Based on Highly-Pure Nanopowders Prepared by DC Reactive Magnetron Sputtering", *Iraqi J. Appl. Phys.*, 16(3) (2020) 27-32.
[20] R.H. Turki and M.A. Hameed, "Spectral and Electrical Characteristics of Nanostructured NiO/TiO_2 Heterojunction Fabricated by DC Reactive Magnetron Sputtering", *Iraqi J. Appl. Phys.*, 16(3) (2020) 39-42.
[21] M.A. Hameed, S.H. Faisal, R.H. Turki, "Characterization of Multilayer Highly-Pure Metal Oxide Structures Prepared by DC Reactive Magnetron Sputtering Technique", *Iraqi J. Appl. Phys.*, 16(4) (2020) 25-30.
[22] N.H. Mutesher and F.J. Kadhim, "Comparative Study of Structural and Optical Properties of Silicon Dioxide Nanoparticles Prepared by DC Reactive Sputtering and Sol-Gel Route", *Iraqi J. Appl. Phys.*, 17(1) (2021) 17-20.
[23] A.M. Hameed and M.A. Hameed, "Highly-Pure Nanostructured Metal Oxide Multilayer Structure Prepared by DC Reactive Magnetron Sputtering Technique", *Iraqi J. Appl. Phys.*, 18(4) (2022) 9-14.
[24] N.A.H. Hashim and F.J. Kadhim, "Structural and Optical Characteristics of Co_3O_4 Nanostructures Prepared by DC Reactive Magnetron Sputtering", *Iraqi J. Appl. Phys.*, 18(4) (2022) 31-36.
[25] A.M. Hameed and M.A. Hameed, "Spectroscopic characteristics of highly pure metal oxide nanostructures prepared by DC reactive magnetron sputtering technique", *Emerg. Mater.*, 6 (2022) 627-633.
[26] N.A.H. Hashim, F.J. Kadhim and Z.S. Abdulsattar, "Characterization of Electrochromism and Photoelectrochromism of N-Doped TiO_2 and Co_3O_4 Thin Films Prepared by DC Reactive Magnetron Sputtering: Comparative Study", *Iraqi J. Appl. Phys.*, 19(1) (2023) 5-12.
[27] S. Saipriya, M. Sultan and R. Singh, "Effect of environment and heat treatment on the optical properties of RF-sputtered SnO_2 thin films", *Physica B: Cond. Matter*, 406(4) (2011) 812-817.
[28] Y. Huang, Y. Zhang and X. Hu, "Structural, morphological and electrochromic properties of Nb_2O_5 films deposited by reactive sputtering", *Sol. Ener. Mater. Sol. Cells*, 77(2) (2003) 155-162.
[29] S.B. Ogale, T.V. Venkatesan and M. Blamire, eds., "Functional metal oxides: new science and novel applications", John Wiley & Sons (2013).
[30] K. Wasa, I. Kanno and H. Kotera, eds., "Handbook of sputter deposition technology: fundamentals and applications for functional thin films", Nano-materials and MEMS, William Andrew (2012).
[31] A.A. Atta et al., "Effect of thermal annealing on structural, optical and electrical properties of transparent Nb_2O_5 thin films", *Mater. Today Commun.*, 13 (2017) 112-118.
[32] K. Huang et al., "Nanoscale conductive niobium oxides made through low temperature phase transformation for electrocatalyst support", *RSC Adv.*, 4(19) (2014) 9701-9708.
[33] M.K. Ali and F.J. Kadhim, "Structural Characteristics of TiO_2/TiN Nanocomposites Synthesized by DC Reactive Magnetron Sputtering Technique", *Iraqi J. Appl. Phys.*, 19(3A) (2023) 49-54.
[34] D.A. Taher and M.A. Hameed, "Spectroscopic Characteristics of Silicon Nitride Thin Films Prepared by DC Reactive Sputtering Using Silicon targets with Different Types of Conductivity", *Iraqi J. Appl. Phys.*, 19(4A) (2023) 73-76.

[35] M. Manzoor et al., "Structural, optical, and magnetic study of Ni-doped TiO_2 nanoparticles synthesized by sol–gel method", *Int. Nano Lett.*, 8 (2018) 1-8.
[36] E.A. Davis and N. Mott, "Conduction in non-crystalline systems V. Conductivity, optical absorption and photoconductivity in amorphous semiconductors", *Philos. Mag.*, 22(179) (1970) 0903-0922.
[37] Z. Li and C. Wang, "One-dimensional nanostructures: electrospinning technique and unique nanofibers", Springer Berlin Heidelberg (NY, 2013).
[38] C.J. Thompson et al., "Effects of parameters on nanofiber diameter determined from electrospinning model", *Polymer*, 48(23) (2007) 6913-6922.
[39] M. Afzali, A. Mostafavi and T. Shamspur, "Electrospun composite nanofibers of poly vinyl pyrrolidone and zinc oxide nanoparticles modified carbon paste electrode for electrochemical detection of curcumin", *Mater. Sci. Eng. C*, 68 (2016) 789-797.
[40] E.T. Salim and H.T. Halboos, "Synthesis and physical properties of Ag doped niobium pentoxide thin films for Ag–Nb_2O_5/Si heterojunction device", Materi. Res. Exp., 6(6) (2019) 066401.
[41] N. Usha et al., "Niobium pentoxide (Nb_2O_5) thin films: rf Power and substrate temperature induced changes in physical properties", *Optik*, 126(19) (2015) 1945-1950.
[42] R. Dangi et al., "Effect of Oxygen Vacancy on the Crystallinity and Optical Band Gap in Tin Oxide Thin Film", *Energies*, 16(6) (2023) 2653.
[43] J. Crank, "The mathematics of diffusion", Oxford University Press (Oxford, 1975).
[44] J. Venables, "Introduction to surface and thin film processes", Cambridge University Press (2000).
[45] D.A. Taher and M.A. Hameed, "Structural and Hardness Characteristics of Silicon Nitride Thin Films Deposited on Metallic Substrates by DC Reactive Sputtering Technique", *Silicon*, 15 (2023) 7855-7864.E.T. Salim et al., "Electrical conductivity inversion for Nb_2O_5 nanostructure thin films at different temperatures", *Mater. Res. Exp.*, 6(12) (2020) 126459.
[46] N. Usha et al., "Effect of substrate temperature on the properties of Nb_2O_5:MoO_3 (90:10) thin films prepared by rf magnetron sputtering technique", *J. Alloys Comp.*, 649 (2015) 112-121.
[47] S.A. Hamdan, "Synthesized pure cobalt oxide nanostructure and doped with yttrium by hydrothermal method for photodetector applications", *Iraqi J. Phys.*, 17(40) (2019) 77-87.
[48] Z. Zhang et al., "Electrospinning of Ag Nanowires/polyvinyl alcohol hybrid nanofibers for their antibacterial properties", *Mater. Sci. Eng. C*, 78 (2017) 706-714.

Table (1) XRD parameters for Nb_2O_5 thin films deposited by different substrate temperatures

T_S (°C)	2θ (Deg.)	FWHM (Deg.)	Relative Int.	d_{hkl} Exp.(Å)	D (nm)	d_{hkl} Std.(Å)	hkl
RT	22.4312	0.3727	100.0	3.9604	21.7	3.9300	(001)
	28.8199	0.4259	10.6	3.0953	19.3	3.1200	(100)
	36.8057	0.6110	5.6	2.4400	13.7	2.4460	(101)
	46.0958	0.4259	11.3	1.9676	20.3	1.9620	(002)
100	22.3834	0.3368	100.0	3.9687	24.0	3.9300	(001)
	28.8083	0.4182	6.9	3.0966	19.6	3.1200	(100)
	36.7358	0.4922	4.4	2.4445	17.0	2.4460	(101)
	46.1917	0.4145	11.2	1.9637	20.8	1.9620	(002)
150	22.3834	0.3109	100.0	3.9687	26.0	3.9300	(001)
	28.5233	0.3959	11.0	3.1268	20.7	3.1200	(100)
	36.7617	0.4440	7.6	2.4428	18.9	2.4460	(101)
	46.1140	0.4100	9.3	1.9668	21.1	1.9620	(002)

